2020

Evaluation of the Activity of Zn-65 Isotope and Radiation Dose Delivered to Drosophila melanogaster

Wasiu Ajani Erinoso
Minnesota State University, Mankato

EVALUATION OF THE ACTIVITY OF Zn-65 ISOTOPE AND RADIATION DOSE DELIVERED TO DROSOPHILA MELANOGASTER

by

Wasiu Ajani Erinoso

A thesis submitted in partial fulfilment of the requirements for Master of Science in Physics

Minnesota State University, Mankato

July 2020

Date: July 10, 2020

Evaluation of The Activity of Zn-65 Isotope and Radiation Dose Delivered to Drosophila Melanogaster

This thesis has been examined and approved.

Examining Committee

Dr. Andrew Roberts_____
Advisor

Dr. Analía Dall'Asén_____
Committee member

Dr. Daniel Toma_____
Committee member

Acknowledgements

I thank Almighty God for His grace and mercy over me. My profound gratitude goes to Dr. Andrew Roberts for introducing me to this research, lending me some of his textbooks, and guiding me throughout my entire days at Minnesota State University, Mankato. I would also like to thank Dr. Thomas Brown, and Dr. Igor Kogoutiouk for their support during my entire days in the department.

I thank Dr. Analía Dall'Asén for her contributions, efforts, and tremendous help. My worthy praise also goes to Dr. Daniel Toma who has been collaborating with us to make this work a success. I would like to extend my gratitude to Mike Peters for all his technical assistance and support. I would also thank Dr. Jorge Méndez, Dr. Hi-Sheng Wu, and Cindy Flitter for their support. My appreciation also goes to all the faculty in the Physics and Astronomy department.

I could not have gone this far without the support of my family, especially my mother Risikat Abeni, dad Alani Isiaka, and siblings. They have always been there for me at all time financially, emotionally, and psychologically.

Lastly, I would like to thank my friends Sodiq Tijani, Vincent Nwachukwu, Ayomikun Orukotan, Tomide Oloruntobi, Abimbola Kolebaje, and all the graduate and undergraduate students in the physics department especially Henri Lemieux for their support.

Abstract

Evaluation of The Activity of Zn-65 Isotope and Radiation Dose Delivered to Drosophila Melanogaster

Wasiu Ajani Erinoso
Master of Science, Physics
Minnesota State University, Mankato
Mankato, Minnesota
July 2020

Radioactivity is a natural part of our environment. Ionizing radiation from radioactive materials can affect the life cycle of organisms; sometimes increase the rate of transition between cycle leading to the proliferation of cells as seen in some cancer cells or delay the rate of transition between cell cycle. A NaI detector is essential to determine the activity of a radioactive material.

To determine the resolution of NaI detector and the efficiency of the geometry used for this experiment, quality control was done for NaI detector using ^{22}Na reference source. The efficiency of the detector was used to verify the activity of ^{65}Zn sample source which was used to irradiate Drosophila melanogaster. Dose rate at points close to ^{65}Zn was calculated and also measured using thermoluminescent dosimeters. The cumulative average dose over the tubes containing fruit flies was also evaluated.

It was discovered that both the resolution and efficiency of the detector decreases with the increase in photon energy. The detector resolution was found to be 13 ± 1 % at

511 keV, and 6.92 ± 0.04 at 1275 keV. At 511 keV the efficiency was 0.02 and at 1275 keV, the efficiency was 0.00712. The calculated and experimental values of ^{65}Zn activity were 38.33 MBq and 37.36 MBq respectively, with 2.5 % difference. At 2 cm and 10 cm away from ^{65}Zn, the measured and calculated dose rates were very close with 3.7 % and 1.8 % differences. The percentage difference in the dose rates from online radprocalculator and experimental values at 2 cm and 10 cm were 35 % and 26.6 % respectively. The average dose to all generations of fruit flies was 160 ±10 rad.

The activity of ^{65}Zn calculated using the detector's efficiency value was very close to the value calculated using the manufacturer's value. The online radprocalculator should be reviewed to accommodate for X-rays from the radioactive samples for points close to the sample. Investigation into the gene expression and inquiries into physical and behavioral changes, life span, and resistance to stress of the offspring of the irradiated flies should be done.

Contents

LIST OF FIGURES

LIST OF TABLES

CHAPTER ONE

INTRODUCTION

1.1 Background of the Study

Radioactivity is a natural part of our environment. In radioactive processes, particles or electromagnetic radiation are emitted from the nucleus. The most common forms of radiation emitted have been traditionally classified as alpha (α), beta (β), and gamma (ɣ) radiation. Nuclear radiation occurs in other forms, including the emission of protons or neutrons or spontaneous fission of a massive nucleus. Of the nuclei found on Earth, the vast majority is stable. This is because almost all short-lived radioactive nuclei have decayed during the history of the Earth. There are approximately 270 stable isotopes and 50 naturally occurring radioisotopes, thousands of other radioisotopes have been made in the laboratory. Unstable atomic nuclei will spontaneously decompose to form nuclei with higher stability. Radioactive decay will change one nucleus to another, the product nucleus has a greater nuclear binding energy than the initial decaying nucleus. The difference in binding energy (comparing the before and after states) determines which decays are energetically possible and which are not. The excess binding energy appears as kinetic energy or rest mass-energy of the decay products.

Throughout the history of living systems, the natural background radiation of the Earth and cosmic rays have been one of the key environmental factors that have affected the rate of evolutionary processes (Moller and Mousseau 2013,

Shahbazi-Gahrouei, Gholami and Setavandeh 2013). Ionizing radiation can influence germ cells causing damage to the DNA and mutations. This can result from the direct and indirect effects of radiation. Ionizing radiation can also affect the life cycle of organisms; sometimes increase the rate of transition between cycle leading to the proliferation of cells as seen in some cancer cells, or delay the rate of transition between cell cycle, this violates the mechanism of cell cycle regulations.

Individuals are frequently exposed to ionizing radiation (IR) from diagnostic, therapeutic, occupational, and environmental sources. Health risks associated with exposure to low-dose radiation (LDR) have been estimated by extrapolating empirical linear fits for data on humans exposed to relatively high doses, however, these results are not sufficient as there are deviations from the dose-dependent linear graph at low doses. A limited understanding of the biological effects induced by ionizing radiation at a low dose/dose rate continues to be the major challenge in predicting radiation risk to human health, because it has various long-term biological effects such as adaptive responses (Ikushima, Aritomi and Morisita 1996) and low-dose hyper-radio-sensitivity (Marples, Wouters and et 2004), in addition to reported beneficial effects (Ina, Tanooka and Yamada 2005). Therefore, it is difficult to evaluate and understand the biological effects of LDR. The biological effects of ionizing radiation can vary depending on the radiation dose (cumulative amount of energy) and dose rate (amount of energy per time).

In low-dose radiation, direct effects of irradiation such as clustered DNA damage and DNA double-strand breaks are minimal, while indirect DNA damages

caused by the induction of reactive oxygen species are very common. The effects in low doses are stochastic, nonlinear on the dose, and depend mainly on the efficiency of the stress response's protective mechanisms. Although it is reasonable to assume that radiation damage to DNA and other cellular machinery is linear as a function of radiation dosage, actual damage is mitigated by cellular repair mechanisms. These repair mechanisms probably increase initially, then reach a maximum so that, depending on parameters, various non-linear curves are possible. It may even be that there is a protective effect due to increased damage response to small amounts of radiation or other types of biological stress.

In the case of high dose radiation, direct effects of irradiation such as the clustered DNA damage, DNA double-strand break, and cell death are major effects and very common. The adverse effects accumulate in the tissues in a deterministic manner that depends linearly on the dose. Many studies related to high-dose radiation have focused on the harmful effects of irradiation, including increase incidence of malignant tumors and developmental abnormalities (O'Driscoll and Jeggo 2006, Tubianna 2009, Weizman, Shiloh and Barzilai 2003).

Ionizing radiation also affects the offspring of exposed parent. One of the consequences of irradiation in the offspring of exposed parents is an increase in the level of embryonic mortality, called dominant lethal mutations which leads to changes in the genetic structure. The protection of the environment and living things from the effects of ionizing radiation has become a key subject for all

relevant international organizations in the field of radiation protection (Keum, et al. 2010).

1.2 Objectives

The goals of this paper are to calculate radiation dose rate at several distances away from ^{65}Zn source and to investigate the biological effects of low dose radiation using *Drosophila melanogaster* as a model organism, focusing on the reproductive cycle of *Drosophila melanogaster*. Important questions are:

(1) is the manufacturer's activity of ^{65}Zn correct?

(2) what is the dose rate at a point close to ^{65}Zn and cumulative dose to the fruit flies for the duration of exposure?

1.3 Significance of the study

Individuals are exposed to LDR through medical procedures, air travel, background exposure, and industrial activities. There has been a surge in the use of radioactive materials over the years in industries, laboratories, hospitals, and schools. Consequently, radioactive contamination of the environment has increased with an increase in the population of individuals exposed to LDR. Also, many radiation workers are unavoidably exposed to prolong LDR, hence, it is increasingly important to evaluate the biological effects of LDR on successive generations of human beings.

1.4 Justification

Drosophila melanogaster is a well-established model organism for genetic studies on development, aging (Parashar, et al. 2008) and longevity (Paaby and Schmidt 2009), and its genes share extensive homology with vertebrate counterparts (Bier 2005). *Drosophila melanogaster* has rapid development and relatively short life span, and it has been used to study the molecular mechanisms of a wide range of human diseases such as neurodegenerative disorders, cardiovascular diseases, kidney diseases, cancer and many more. Drosophila has comparable radiosensitivity to mammals in the preimaginal stages (Nakamura, Suyama, et al. 2013). At the same time, adult individuals, due to the postmitotic state of most tissues, are about 100 times more radioresistant (Ogaki and Nakashima-Tanaka 1966). It has advantages in experimental design due to easier scaling up and reproduction than many other organisms. Considerable progress in understanding life-span regulation has been achieved during the last two decades based on work in *Drosophila*; oxidative stress, food restriction, heat shock, and ionizing radiation can modulate life span (Moskalev, Plyusnina and Shaposhnikov 2011). *Drosophila* larvae have an intricate peripheral nervous system that detects odors, light, temperature, sound, and mechanical touch, enabling the study of sensory signaling (Johnson and Carder 2012). Therefore, *Drosophila melanogaster* is an ideal model for LDR research.

CHAPTER TWO

LITERATURE REVIEW

2.1 Zinc Isotopes (65Zn) Atom

Naturally occurring Zinc $_{30}Zn$ has five stable isotopes, ^{64}Zn, ^{66}Zn, ^{67}Zn, ^{68}Zn, and ^{70}Zn with ^{64}Zn being the most abundant (48.6% natural abundance). Twenty-five radioisotopes have been characterized with the most abundant and stable being ^{65}Zn with a half-life of 244.26 days, and ^{72}Zn with a half-life of 46.5 hours. All of the remaining radioactive isotopes have half-lives that are less than 14 hours and the majority of these have half-lives that are less than 1 second. This element also has 10 meta states.

Zinc has been proposed as a "salting" material for nuclear weapons. A jacket of isotopically enriched ^{64}Zn, irradiated by the intense high-energy neutron flux from an exploding thermonuclear weapon, would transmute into the radioactive isotope ^{65}Zn with a half-life of 244 days and produce approximately 1.115 MeV (Roost, et al. 1972) of gamma radiation, significantly increasing the radioactivity of the weapon's fallout for several days. Such a weapon is not known to have ever been built, tested, or used (Win and Masum 2003).

Zinc-65 atom is a zinc atom in which the nucleus has **35** neutrons. It has a half-life of 244 days, decaying by the emission of a positron (beta (+) decay), and

is the most abundant and stable of the 25 known radioisotopes of zinc. Because of these characteristics ^{65}Zn was chosen for this research.

2.2 Radiation dose measurement and management

Dose rate meters are the most widely used, and perhaps one of the most important tools for the measurement of ionizing radiation. They are often the first, or only device available to a user for an instant check of radiation dose at a certain location. Throughout the world, radiation safety practices rely strongly on the output of these dose rate meters. Measuring radiation essentially means measuring the amount of radiation that an object absorbs. This is termed absorbed dose, and the international system of units (SI unit) is Gy (gray). In the past, the rad (radiation absorbed dose) unit has also been used (FDA 2015). The SI unit for radioactive material representing radioactivity is Bq (Becquerel). One Bq is defined as the activity of a quantity of radioactive material in which one nucleus decays per second. The Bq unit is equivalent to an inverse second. The becquerel succeeded the curie (Ci), an older, non-SI unit of radioactivity defined as 3.7×10^{10} nucleus decay per second. Hence, 1 Ci = 3.7×10^{10} Bq (FDA 2015). The reason radiation is of interest to us is because of its potential effect on the human body. To represent this biological effect, the Sv (sievert) unit is used. Sv represents the biological effect on the human body regardless of the type of radiation used. Neutron and alpha radiation can cause increased biological harmful effects. These increased effects are reflected in rem (roentgen equivalent man) units. To represent smaller effects,

mSv (millisievert) units representing 1/1,000 of a Sv are used. In the past rem (roentgen equivalent man) was used. For practical purposes, 1 rem can be thought of as 1 roentgen, and 1 mSv is equal to 100 mrem. It is important to know the concepts of exposure dose, absorbed dose, equivalent dose, and effective dose (ICRP 1991, FDA 2015, ICRP 2007).

2.2.1 Exposure

Exposure describes the strength of gamma and X-rays from a certain location, which determines the amount ionization possible in the air. Exposure is only used when gamma or X-rays are used in air, and not when other radiation types or other materials are radiated. The unit used in the past was Roentgen (R) and it is currently Coulomb/kilogram (C/kg). 1 R is the radiation needed to create 2.58×10^{-4} C in 1 kg of air.

2.2.2 Absorbed dose

Absorbed dose is defined as the energy of ionizing radiation absorbed per unit mass by a body, often measured in Gy (gray). 1 Gy is defined as the absorption of one joule of radiation energy per one kilogram of matter. In the past, rad units were used, with 1 rad equal to 1/100 J/kg, which is equal to 1/100 Gy. Absorbed dose is used regardless of radiation type or radiated material.

2.2.3 Equivalent dose (uniform dose exposure to a single organ or whole-body)

Neutrons, alpha particles, and energic ions have different effects of damage when compared with X-ray or gamma particles. Also, the damage varies by area irradiated in the human body. Absorbed dose and equivalent dose have the following relationship; Equivalent dose is equal to absorbed dose multiplied by the radiation weighting factor. The International Commission for Radiological Protection (ICRP) 103 recommended radiation weighting factors (ICRP 2007). When using Gy units as absorbed dose the resulting equivalent dose unit is Sv. The radiation weighting factor for X-rays and gamma rays is 1.0, and this results in an equivalent dose unit of Sv, but this practice is discouraged as it can lead to confusion with effective dose. In the past rem units were also used with 100 rem equal to 1 Sv.

2.2.4 Effective dose

An effective dose is defined as the tissue-weighted sum of all equivalent doses in all parts of the body representing stochastic health risk, which is the probability of cancer induction and harmful genetic effects of ionizing radiation. This is because the same radiation can have varying effects according to different parts of the body. The body is divided into different organs. An effective dose is equal to the sum of the equivalent dose by each organ multiplied by the tissue weighting factor of each organ. The ICRP 103 recommended tissue weighting factors (ICRP 2007) and notice that the sum of tissue weighting factors is 1.0, which

represents the weighting factor for whole-body exposure. The unit used is Sv which is the same as the equivalent dose. Exposure to 1 R of gamma or X-ray leads to 1cGy of absorbed dose, and when the whole body is uniformly exposed, leads to 1 cSv of effective dose. When comparing using lay man's terms, exposure can be thought of as "How much is it raining?", absorbed dose as "How much did you get wet?", and estimated dose as "What are the chances of getting cold due to getting wet in the rain?".

2.3 Conventional interactions of ionizing radiation with biological matter

Ionizing radiation is energetic and penetrating. Many of its chemical effects in the biological matter are due to the geometry of the initial physical energy deposition events, referred to as the track structure. Ionizing radiation exists in either particulate or electromagnetic types. The particulate radiation interacts with the biological tissue either by ionization or excitation. The ionization and excitation that it produced tend to be localized, along the tracks of individual charged particles. Whereas the photon can penetrate matter without interacting, it can be completely absorbed by depositing its energy, or it can be scattered (deflected) from its original direction and deposit part of its energy as follows:

1. Photoelectric interaction: a photon transfers all its energy to an electron located in one of the atomic shells, usually the outer shell. The electron is ejected from the atom and begins to pass through the surrounding matter.
2. Compton scattering: only a portion of the photon energy is absorbed and a photon is scattered with reduced energy. The photon that is produced leaves in a different direction than that of the original photon with a different energy.
3. Pair production: the photon interacts with the nucleus in such a way that its energy is converted to matter producing a pair of particles, an electron (negatively charged particle), and a positron (positively charged particle). This only occurs with photons with energies of more than 1.02 MeV (Hall and Giaccia 2011).

2.3.1 Direct effect

In the direct action, the radiation hits the DNA molecule directly, disrupting the molecular structure. Such structural change leads to cell damage or even cell death. Damaged cells that survive may later induce carcinogenesis or other abnormalities. This process becomes predominant with high linear energy transfer radiations such as α-particles and neutrons, and high radiation doses. This is shown in figure 2.1.

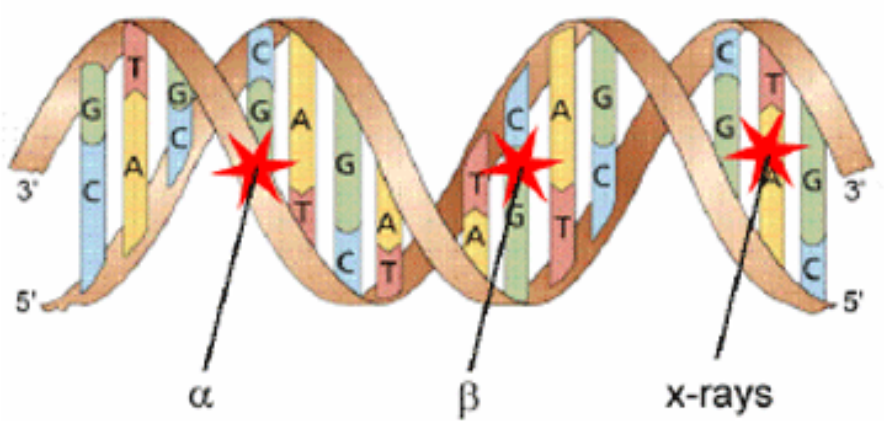

Figure 2.1 Direct radiation damage to cells

2.3.2 Indirect effect

In the indirect action, the radiation hits the water molecules, the major constituent of the cell, and other organic molecules in the cell, whereby free radicals such as hydroxyl (HO) and alkoxy (RO_2) are produced. Free radicals are characterized by an unpaired electron in the structure, which is very reactive and therefore reacts with DNA molecules to cause molecular structural damage. Hydrogen peroxide (H_2O_2) is also toxic to the DNA molecule. The result of the indirect action of radiation on DNA molecules is the impairment of function or death of the cell. The number of free radicals produced by ionizing

radiation depends on the total dose. It has been found that the majority of radiation-induced damage results from the indirect action mechanism because water constitutes nearly 70% of the composition of the cell (Saha 2013). In addition to the damages caused by water radiolysis products, cellular damage may also involve reactive nitrogen species (RNS) and other species (Wardman 2009), and can occur also as a result of ionization of atoms on constitutive key molecules (e.g. DNA) as shown in figure 4.2.

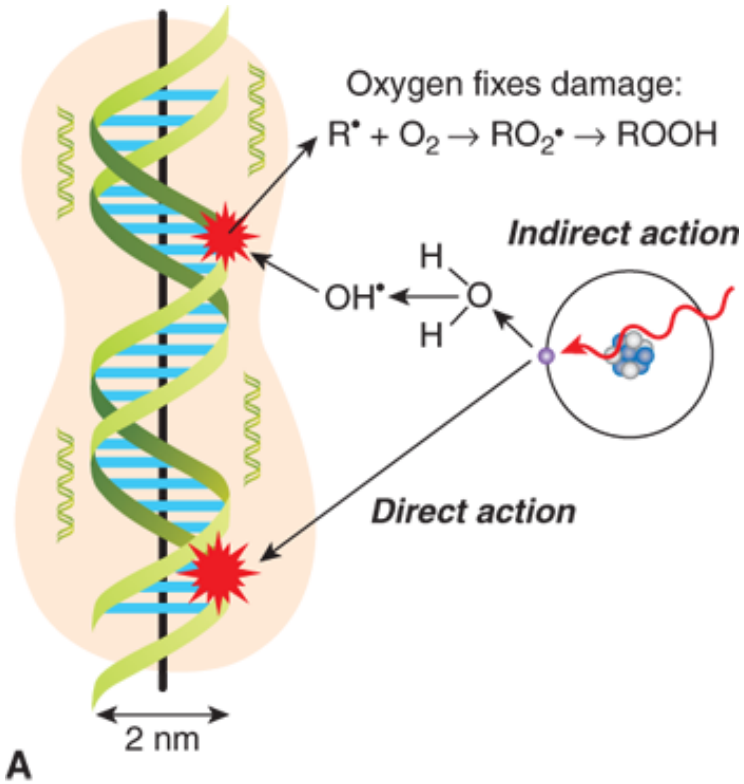

Figure 2.2: Indirect radiation damage to cell

The ultimate result, of direct and indirect effects, is the development of biological and physiological alterations that may manifest themselves seconds or decades later. Genetic and epigenetic changes may be involved in the evolution of these alterations (Koturbash, et al. 2008).

2.4 Effects of ionizing radiation on cells

The danger of ionizing radiation on human health is well known since the discovery of radioactivity and X-rays. There is a general agreement that high doses of ionizing radiation represent a major threat to human health. Radiation damage to the cell can be caused by the direct or indirect action of radiation on the DNA molecules. When a cell is hit, the deposition of energy can result in direct damage to the genetic material or indirect damage to critical nuclear targets through the radiolysis of water.

Many scientists have expressed growing doubts and proposed different models concerning the risks linked to persistent exposures to small doses of ionizing radiations, which are much more frequent than accidental exposure to high doses. These potential risks could recognize new biological mechanisms of damage, including epigenetic, procarcinogenic pathways, and transgenerational

transmission. Stem cells reside for a long time in our bodies, and this increases the probability that they accumulate genotoxic damage, from extrinsic or intrinsic sources. Following damage, cells may properly repair DNA and re-establish functionality, but if DNA damage is extensive, cells may accumulate irreversible damages that trigger either apoptosis or senescence. Alternatively, cells with unrepaired damage may sustain mutations and undergo malignant transformation (Rando 2006). On these premises, stem cells may be the major target to assess the low dose of ionizing radiation effects. Because of their long life, stem cells may sustain several rounds of low-level radiation damage that, taken singly, may not have a big impact on cellular physiology, but collectively, these rounds of radiation damage may severely affect cellular function (Alession, Gaudio and Capasso 2015). Accordingly, alteration in quality and/or quantity of tissue stem cells may be considered as a predictive risk indicator for future health hazards (Prise and Saran 2011). In addition to cancer, available data indicates that low dose ionizing radiation can be associated with cataracts, cardiovascular disease, and long-term psychological consequences (Ainsbury, Bouffler and Dorr 2009).

Contrarily, some studies report that low dose ionizing radiation also can induce beneficial effects in humans, such as hormesis and adaptive responses, fueling the debate on the effects of low dose ionizing radiation (Tang and Loke 2015). Hormesis is a two steps dose-response to an environmental factor. It presents a low dose stimulation or favorable effect and a high dose toxic effect (Mattson

2008). There is experimental evidence that low dose ionizing radiation also induces defensive responses such as detoxification of reactive oxygen species (ROS), high-fidelity repair of DNA damage, protection from spontaneous mutation occurrence in-vivo, and protection from spontaneous neoplastic transformation occurrence in-vitro (Rothkamm and Lobrich 2003).

The adaptive response is defined as the result of a very low priming dose of radiation stimulating cellular processes that result in enhanced resistance to a second larger dose of ionizing radiation that induces DNA damage (Tang and Loke 2015).This response involves the activation of numerous signaling pathways (Coleman, Yin and Peterson 2005). Evidence suggests that cells responded to ionizing radiation by the activation of genes associated with DNA repair, stress, cell cycle control, and apoptosis. Besides, low dose ionizing radiation can also induce “bystander” effects: irradiated cells could signal their distress to healthy cells, either by direct cell-to-cell interaction or by paracrine signaling (Bonner 2003).

2.5 Radiation Protection

Radiological protection is a science-based discipline in which concepts, methods, and procedures are developed to be used for the protection of humans and the environment from the harmful effects of ionizing radiation. Specifically, radiological protection has the objective of reducing the likelihood of radiation-induced stochastic effects, in particular, cancer and preventing deterministic

effects. Almost all regulatory requirements authorizing activities that use ionizing radiation such as in industry, health, agriculture, and basic research, is based on the radiation protection concept that hinges on the acceptance of the linear non-threshold (LNT) theory.

LNT implies that any dose, no matter how low, can pose risks for genetic (hereditary) defects or cause cancer. Cancer risk is assumed to increase linearly with increasing radiation dose, with no threshold. LNT was derived using a statistically significant dose-response (DR) relationship between radiation dose received by the survivors of the atomic bomb explosions in Hiroshima and Nagasaki and the observed health effects, mainly hereditary disorders and cancer (decades later, non-cancer risks are also derived from the same population).

The LNT model is being challenged particularly in relation to the environment because it is now clear that at low doses are of concern in radiation protection, cells, tissues, and organisms respond to radiation by inducing responses that are not readily predictable by dose. These include adaptive responses, bystander effects, genomic instability, and low dose hypersensitivity. The phenomena contribute to observed radiation responses and appear to be influenced by genetic, epigenetic, and environmental factors, meaning that dose and response are not simply related and the modeling of dose-response relationships based on the number of irradiated cells may not be a valid approach (Little 2003).

ICRP in its new review 2007, considered possible challenges to its linear non-threshold model but concluded that for radiological protection, it is

scientifically reasonable to assume that the incidence of cancer or hereditary disorders will rise in *direct proportion* to an increase in the equivalent dose in the relevant organs and tissues, below about 100 mSv. ICRP also considered issues such as cellular adaptive responses, genomic instability, and bystander signaling but notes that 'since the estimation of nominal cancer risk coefficients is based upon direct human epidemiological data, any contribution from these biological mechanisms would be included in that estimate (Wrixon 2008).

BEIR VII concluded that the available biological and biophysical low dose data support a linear-no-threshold (LNT) risk model. According to this model, even the smallest dose of radiation has the potential to cause a small increase in health risk to humans. The reports from UNSCEAR and the ICRP concluded that the LNT hypothesis remains a prudent basis for radiation protection at low doses and low dose rates, but may not reflect biological differences and risks in the low dose region (Morgan and Bair 2013).

The International Commission for Radiological Protection (ICRP) recommends that medical activities involving ionizing radiation should fulfill the three basic principles of justification, optimization, and application of dose limit (ICRP 2000).

2.5.1 Principles of justification

The principle of justification is that, in general, "any decision that alters the radiation exposure situation should do more good than harm". This means that by

introducing a new radiation source, by reducing existing exposure, or by reducing the risk of potential exposure, one should achieve sufficient individual or societal benefit to offset the detriment it causes (ICRP 2007). The RAND Corporation has developed a definition of "appropriate" that is widely used: the expected health benefit (i.e. increased life expectancy, relief of pain, reduction in anxiety, improved functional capacity) exceeds the expected negative consequences (i.e. mortality, morbidity, the anxiety of anticipating the procedure, pain produced by the procedure, misleading or false diagnoses, time lost from work) by a sufficiently wide margin that the procedure is worth doing (Sistrom 2008). In other words, the anticipated benefits should exceed all anticipated procedural risks, including radiation risk.

2.5.2 Principles of optimization

The principle of optimization of protection is that "the likelihood of incurring exposures, the number of people exposed, and the magnitude of their doses should all be kept low, considering economic and societal factors. This means that the level of protection should be the best under the prevailing circumstances, "maximizing the margin of benefit over harm" (ICRP 2007).

The **"As Low As Reasonably Achievable" (ALARA)** principle is a safety principle, recommended by national and international radiation protection agencies for radiation workers, to address the growing concerns of radiation-induced somatic

and heritable mutations (Prasad, cole and Hasse 2004, Anonymous 1991). The ALARA principle means that every reasonable effort must be made to keep radiation workers and the public, as far below the required limits of radiation, as possible (shaw, Crouail and Drouet 2010). The above three physical principles do have limitations, implying that the ALARA principle may always not be adhered to by radiation workers.

Increasing the distance between the radiation source and exposed individuals may also not be practical for many radiation workers or patients. Reducing exposure time may not be pertinent to all populations, except those that are involved in taking care of patients who have received gamma-emitting radioisotopes for medical purposes or who are responsible for radioactive decontamination as a result of accidents or attacks (Prasad, cole and Hasse 2004).

Prasad *et al* 2004 suggested it would be important to identify biological or chemical agents, which when given before radiation exposure, could protect all normal tissues. Such radio-protective agents would protect patients against radiation damage during diagnostic procedures. The search for radio-protective agents began soon after World War II but the numerous agents identified during extensive radiobiological research have been toxic to humans (Prasad, cole and Hasse 2004, Anne 2002). Prasad *et al* 2002, in a study considering the positive and negative aspects of anti-oxidant use during radiation therapy, found a combination of dietary antioxidants was more effective in normal tissue during radiation therapy than any of the agents used on their own (Prasad, Cole, et al. 2002). Furthermore,

Prasad *et al* 2004, in a review article on radiation protection proposed a combination of dietary antioxidants and glutathione-elevating agents that could be useful in protecting normal tissue against radiation damage, no matter how small the damage might be. The use of antioxidant preparations can extend the concept of ALARA from dose to biological damage for radiation workers. Also, such antioxidants can protect against radiation damage, for patients receiving diagnostic doses. The authors also suggested a clinical study to evaluate the radioprotective value of antioxidants in patients receiving diagnostic radiation, using measures of oxidative stress and frequency of mutations (Prasad, cole and Hasse 2004).

2.6 Drosophila Melanogaster

The fruit fly, *Drosophila melanogaster*, is used as a model organism to study disciplines ranging from fundamental genetics to the development of tissues and organs. *Drosophila* genome is 60% homologous to that of humans, less redundant, and about 75% of the genes responsible for human diseases have homologs in flies (Ugur, Chen and Bellen 2016). These features, together with a brief generation time, low maintenance costs, and the availability of powerful genetic tools, allow the fruit fly to be eligible to study complex pathways relevant in biomedical research, including cancer.

The first documented use of *Drosophila* in the laboratory was by William Castle's group at Harvard in 1901, although the “father” of *Drosophila* research is undoubtedly Thomas Hunt Morgan (Kohler 1994). Morgan greatly refined the

theory of inheritance first proposed by Gregor Mendel, by using *Drosophila* to define genes and establish that they were found within chromosomes (long before it was even established that DNA is the genetic material). Morgan won the Nobel Prize in Physiology or Medicine in 1933 "*for his discoveries concerning the role played by the chromosome in heredity*" (The Nobel Prize in Physiology or Medicine 1933). One of Morgan's protégés, Hermann Muller, won the Nobel Prize in Physiology or Medicine in 1946 "*for the discovery of the production of mutations through X-ray irradiation*" (The nobel prize in Physiology or medicine 1946). Using *Drosophila* in the 1920s, Muller discovered that X-rays caused a massive increase in the mutation rate of genes and could break chromosomes (Muller 1928). Although irradiated flies looked normal, their offspring frequently showed the effects of mutation. This led to the realization that radiation causes harmful genetic defects in the offspring of exposed humans – a timely observation given that this was at the advent of man's attempts to harness and exploit nuclear fission.

Cancer stem cells have more features than tissue stem cells because they can initiate tumor growth and fuel its maintenance and metastasis (Malanchi, et al. 2011, Kreso and Dick 2014). Besides, cancer stem cells are highly resistant to conventional therapy, both radiation and chemotherapy, and they are responsible for the recurrence of disease (Mueller, et al. 2009). Since the mechanisms underlying the ability of stem cells to support cancer progression are still unclear, *Drosophila* is convenient to use as it provides many tools for genetic and

molecular investigations. Adult stem cells are required for tissue homeostasis and repair after injury and in adult flies, populations of stem cells are present in the posterior midgut, testis, and ovarian follicle rendering it again a good system to dissect these stem cell programs (Hou and Singh 2017). *Drosophila* and mammalian stem cells are similar, and they are regulated by homologous signals corroborating the use of the fly in the field of tumor biology.

Moskalev et al. 2007 & 2011, and Seong KM et al. 2011, revealed that relatively low dose exposure (20–75 cGy) of fruit flies on immature preimaginal stages in some cases has long-term effects that lead to an increased life span and resistance to other stresses, such as hyperthermia (Moskalev, Shaposhnikov and Turysheva 2009, Vaiserman, et al. 2003, Seong, et al. 2011). It is known that the preimaginal stages of Drosophila have comparable radio-sensitivity to mammals (Nakamura, et al. 2013). At the same time, adult individuals, due to the postmitotic state of most tissues, are about 100 times more radioresistant (Ogaki and Tanaka 1966). In their work, Antosh et al. 2014, revealed that irradiation of Drosophila individuals in the imago stage in doses from 0.1 to 400 Gy causes a statistically significant effect on lifespan and gene expression only if the dose is higher than 100 Gy (Antosh, et al. 2014). At the same time, in the work of Moskalev et al. 2014, comparing the effects of irradiation in the adult Drosophila male and female at the 20 cGy dose rate, some differentially expressed genes were observed (Moskalev, Shaposhnikov and Snezhkina, et al. 2014).

CHAPTER THREE

MATERIALS AND METHODS

3.1 Sodium Iodide NaI detector

NaI detector is very sensitive to gamma radiation. The high Z of iodine in NaI gives good efficiency for γ-ray detection. When radiation strikes the NaI detector, it converts the ionization and excitation produced by radiation into a light pulse or scintillation. The amount of light that is produced is proportional to the energy deposited by the radiation particle/photon. The small light pulse is converted into an electric pulse by an electric component called photomultiplier tube. The light decay time constant in NaI is about 0.25 μs. The size of the amplified electric pulse is proportional to the energy deposited by the radiation photon/particle. The basic components and operating principle of a scintillation detector are illustrated in figure 3.1.

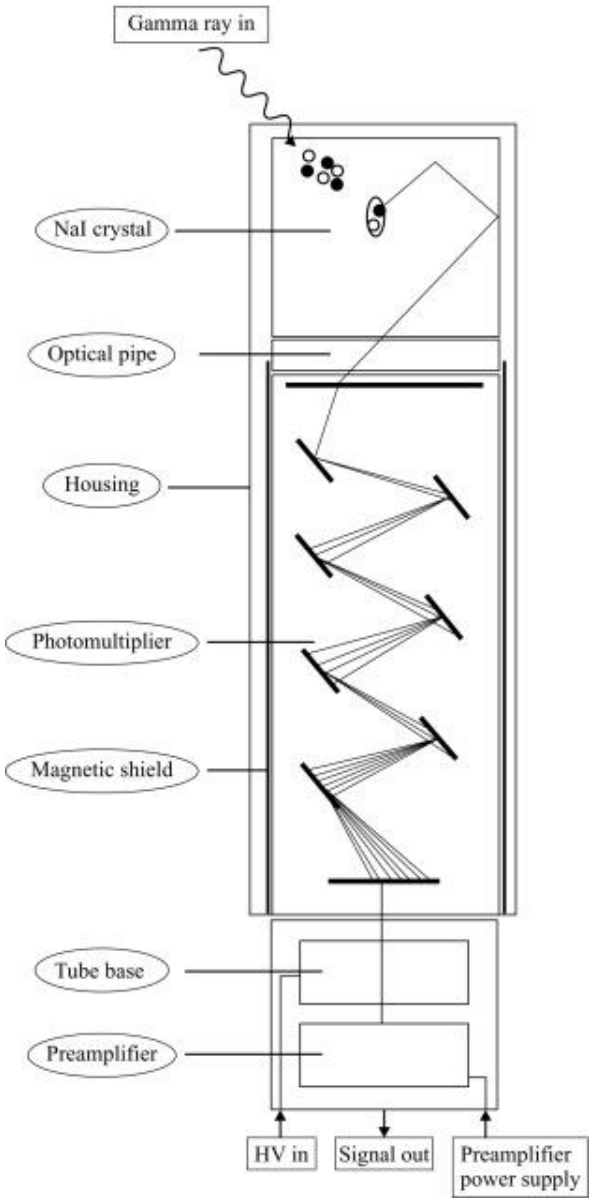

https://web.stanford.edu/group/scintillators/scintillators.html

Figure 3.1. Schematic diagram of operation of scintillation detector

3.1.1 Detector resolution

The detector resolution was evaluated using ^{23}Na reference source with known activity. The resolution is a measure of how narrow the peaks of the graph are. It is commonly measured using the Full Width at Half Maximum (FWHM) which is the width of the photopeak at which the values are ½ the maximum value. Equation 3.1 was used to evaluate the resolution of the detector.

$$R = \frac{E_+ - E_-}{E_o} \, X \, 100 \qquad [3.1]$$

where E_o is the energy at the center of the peak, E_+ is the energy number greater than E_o where the count is half the maximum peak and E_- is the energy lower than E_o where the count is half the maximum peak. $E_+ - E_-$ is called the full width at half maximum which was determined directly from the detector interface software. The uncertainty in the resolution of the detector was found using equation 3.2.

$$\delta R = R \sqrt{\left(\frac{\sqrt{(\delta E_+)^2 + (\delta E_-)^2}}{(E_+ - E_-)}\right)^2 + \left(\frac{\delta E_o}{E_o}\right)^2} \qquad [3.2]$$

3.1.2 Energy calibration of the detector

The channel number of the photo-peak is approximately proportional to the energy of gamma (or X-ray) of the source. The scaling factor is controlled by the amplifier gain. Since there is an exact linear relationship between the channel number and energy, equation 3.3 shows the relationship between the channel number and energy of the gamma-ray.

$$E = \alpha C \quad [3.3]$$

Where e is the energy of the gamma, C is the channel number of the center of the photopeak, and α is the scaling factor with units of energy/channel number.

3.1.3 Detector counting efficiency

The counting efficiency ε of a detector is defined as the ratio of the number of particles detected to the number of particles emitted. Equation 3.4 was used to find the counting efficiency of the detector using ^{22}Na of known activity.

$$\varepsilon = \frac{number\ of\ particles\ detected}{number\ of\ particles\ emitted} \quad [3.4]$$

The *number of particles emitted* was calculated using equation [3.5]. The *number of particles detected* is the background counts subtracted from the sum of all the counts of the gaussian curve centered on an energy.

$$number\ of\ particles\ emitted\ =\ activity\ (Bq)\ *\ yield\ fraction\ *\ time\ (s) \quad [3.5]$$

Efficiency is a number between 0 and 1. The counting efficiency allows us to find the number of particles emitted by the sample when the number of particles detected has been known. Since counting efficiency depends on the source-detector geometry and the size of the detector, the two factors were kept constant throughout the experiment.

3.2 ^{22}Na reference sample

^{22}Na was acquired on December 06, 2008, with an activity of 1.122 μC. ^{22}Na was used as a reference source sample to calibrate the detector. The current

activity of ^{22}Na at the time of use was calculated using equation 3.5. ^{22}Na has half-live of 2.6 years, it produces two gamma energies 0.511 MeV and 1.275 MeV. The highest energy peak at 1.275 MeV is emitted when the ^{22}Na nucleus decays from an excited state. The peak at 0.511 MeV results from positron emission and corresponds to the rest energy of an electron (or positron).

3.3 Activity of ^{65}Zn source

^{65}Zn was procured from the Department of Physics at the University of Wisconsin, Maddison. ^{65}Zn was produced from the nuclear reaction of Copper ^{65}Cu (p,n). It was collected on April 1, 2019, with an initial activity of 70 MBq. It is a flat thin metal folded into a cylindrical shape dimension of 16.40 mm height and 10.61 mm diameter. The source was kept in a cylindrical transparent plastic. The radioactive area of the copper metal was about 0.2829 mm^2 and this geometry was put into consideration when calculating the radiation dose.

3.3.1 Indirect measurement of activity

The activity of the source was calculated when it was first used in our department using the given activity at the time of production using equation [3.6].

$$A = A_0 e^{-\lambda t} \qquad [3.6]$$

where A is the new activity of the source in mega Becquerel (MBq), A_0 is an initial activity of the source 70 MBq, and λ is decay constant, decay constant λ was calculated using equation [3.7].

$$\lambda = \frac{ln2}{t_{1/2}} \quad [3.7]$$

where $t_{1/2}$ is the half-life of ^{65}Zn and is 243.93 days, *t* is time in seconds from April 1, 2019, to the day experiment was carried out.

3.3.2 Direct measurement of activity

The activity of the source was also measured using a sodium iodide (NaI) detector in the Department of Physics and Astronomy at Minnesota State University, Mankato. The detector was shielded with lead block allowing for a narrow path of 4.0-cm wide between the source and the detector, and the source was placed 40 cm from the detector to reduce dead time for both the ^{23}Na and ^{65}Zn sources to maintain consistency.

3.4 Thermoluminescent dosimeters

Thermoluminescent dosimeter, TLD, is a radiation dosimeter used for measuring ionizing radiation exposure by measuring the intensity of light emitted by a crystal inside the detector when the crystal is heated. It contains small chips of lithium fluoride, which absorb ionizing radiation energy as shown in figure 3.2. The radiation interacts with the crystal in the detector causing the electrons in the crystal's atoms to jump to higher energy states, where they get trapped in a metastable state but can be restored to their original ground state by heating. Whereby on heating, the electrons return to their ground state and light is emitted.

The amount of light emitted is related to the dose of radiation absorbed by the TLD and to the radiation exposure dose of the individual.

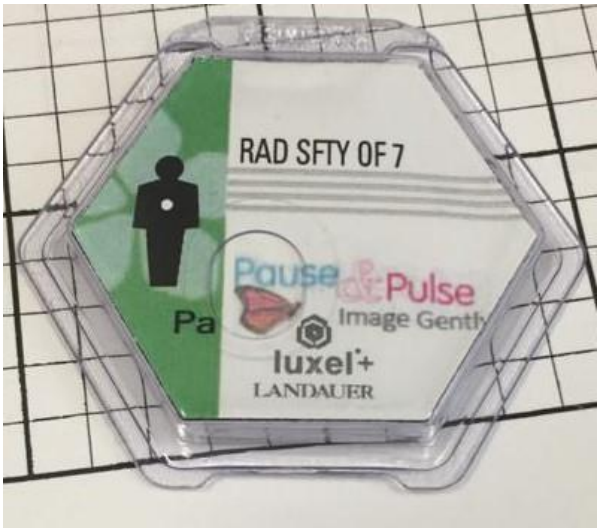

Figure 3.2: Thermoluminescent dosimeter

3.5 Dose measurement

The radiation dose was calculated through direct and indirect measurements. Doses were recorded in rad/hour. The total radiation dose due to all ionizing radiations and particles coming from the ^{65}Zn was measured directly using thermoluminescent dosimeters. The eggs of the fruit flies were placed in test tubes of diameter of 2.6 cm and height of 6.0 cm. For each generation of the fruit flies, there were four test tubes and the tubes were placed to surround the radioactive source in a concentric circle. The tubes were rotated at several intervals to achieve an even dose distribution.

3.5.1 Direct dose measurement from all radiations and particles

Doses were measured using thermoluminescent dosimeters. Two dosimeters were placed 2 cm and 10 cm away from the source from opposite sides for 23 hours. They were both sent to the laboratory for analysis of the dose received within the 23 hours of exposure. The dosimeter placed 2 cm from the source sample was labeled A, while the dosimeter placed 10 cm from the source sample was labeled B as seen in figure 3.3. The dose rate was calculated using equation [3.8].

$$dose\ rate = \frac{measured\ dose}{23} \qquad [3.8]$$

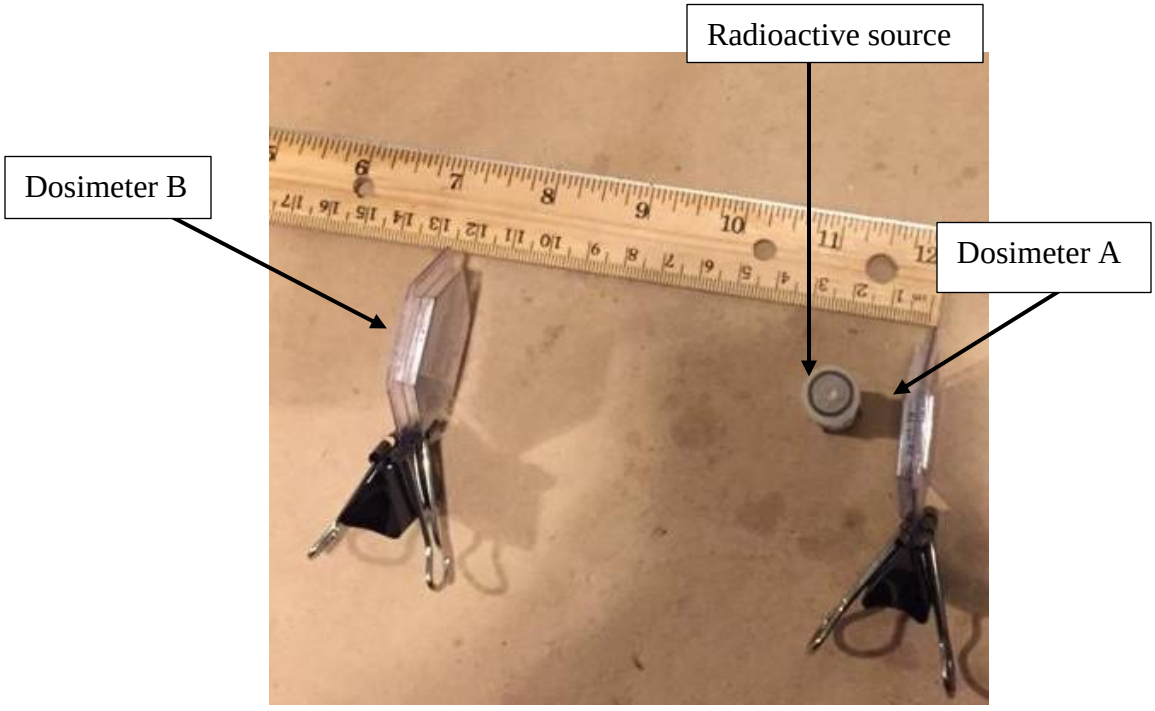

Figure 3.3: Measurement of radiation dose using thermoluminescent dosimeters

3.5.2 Indirect measurement of radiation doses

Doses were calculated using the known and evaluated parameters based on the activity and the percentages of the types of radiation from the source. The dose R was calculated using equation [3.9]

$$R = \frac{0.5\ CEF}{0.877\ r^2} \qquad [3.9]$$

where 0.5 is unit conversion constant and 0.877 is to convert from Roentgen to Rad, R is the dose rate in $\frac{Rad}{hr}$, C is the activities in curies, 1 Curie $= 3.7$ X 10^{10} Bq, E is the energy of photon in megaelectronvolt (MeV), F is the fractional yield of the photon, r is the distance from the source in meters (m).

The activity used for the dose calculation was dependent on the day the experiment was carried out in the laboratory. The average total volume dose delivered to the bugs in the test tube was calculated using equation [3.10].

$$Volume\ dose = \int \frac{0.5\ CEF}{0.877\ r^2}\ dv * time \qquad [3.10]$$

Both the calculated and measured doses were compared to the doses gotten from the Rad Pro Calculator online (http://www.radprocalculator.com/Gamma.aspx). The isotope, source activity, and point of reference-to-source distance were entered into the calculator online and it automatically calculates the dose rate at the reference point.

CHAPTER FOUR

RESULTS AND DISCUSSION

4.1 Sodium iodide (NaI) detector calibration

To determine the spectrum of ^{22}Na, an investigation was made into the background radiation since there were many radioactive sample sources in the laboratory. The detector geometry was kept constant for the background investigation and data was collected for a total of 10 minutes. Figure 4.1 shows the graphical representation of the background counts in the laboratory.

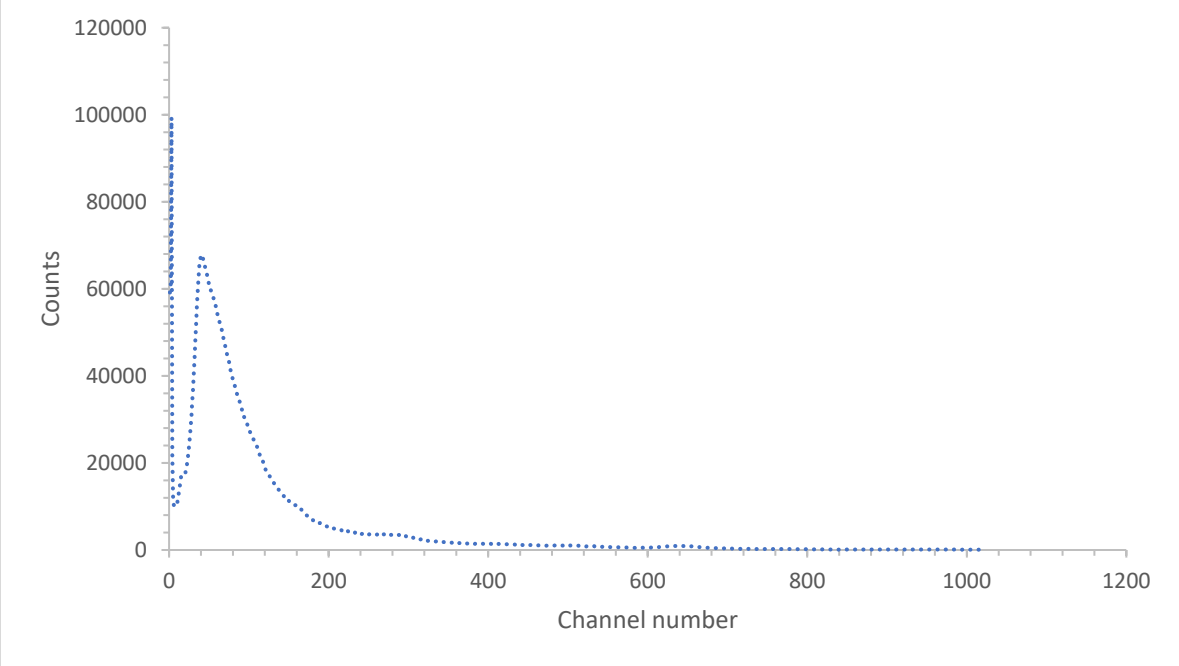

Figure 4.1: Background spectrum

The spectrum shows that there are several low-energy X-rays from some materials in the laboratory. These X-rays might be from some radioactive materials in the laboratory, and characteristic X-rays and bremsstrahlung X-rays from the effects of high-energy gamma radiation striking some nearby materials.

^{22}Na source was positioned 40 cm away from the detector and the detector recorded the spectrum of the unattenuated beam produced by ^{22}Na. The recorded spectrum matches the agreed model for ^{22}Na. The spectrum is presented in figure 4.2 below.

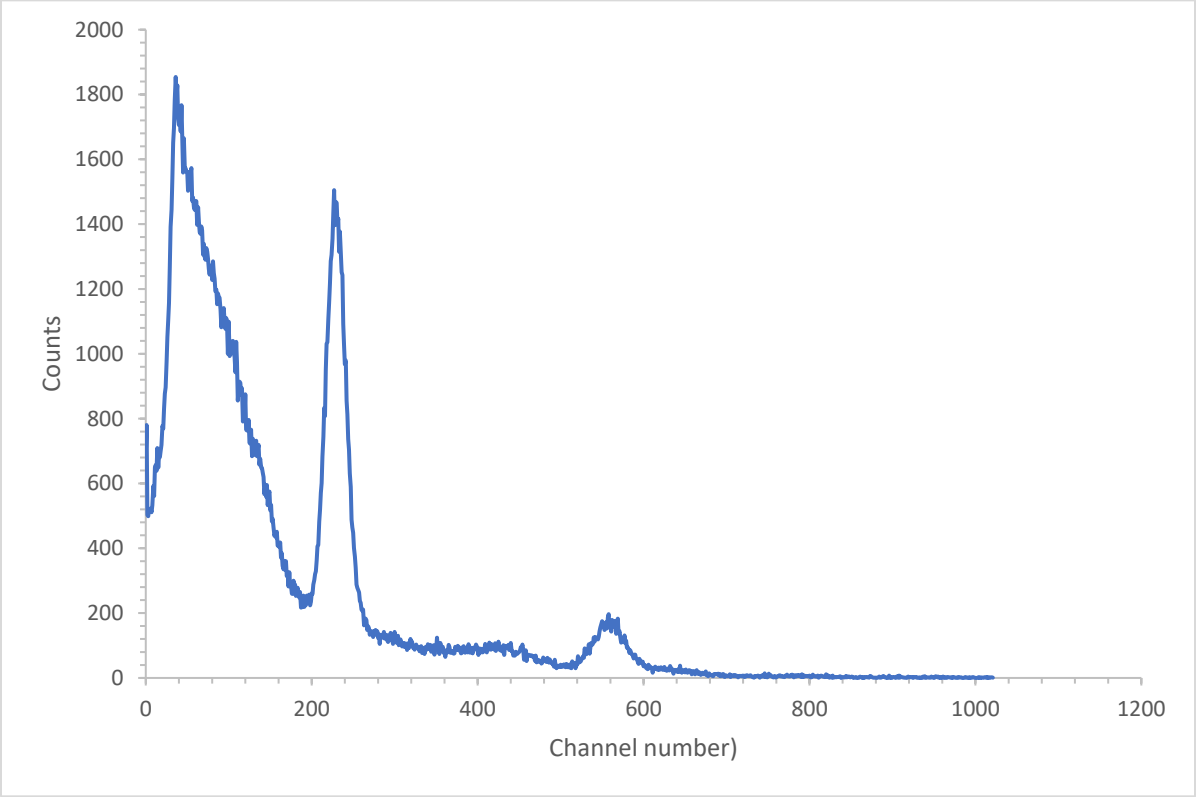

Figure 4.2. Spectrum of ^{22}Na

The first peak results from the Compton edge, backscatter, and background radiation. The Compton edge result from the fact that some of the 0.511 MeV gamma rays from ^{22}Na undergo Compton scattering with electrons in the crystal, losing much of their energy to the electrons. In the extreme case of a head-on collision, the gamma rays are completely backscattered 180 degrees. This results in the backscatter peak predicted by conservation of energy and conservation of momentum (https://www.andrews.edu/phys/wiki/PhysLab/doku.php?id=272s11l12&do= n.d.).

The second peak results from positron emission and corresponds to the rest energy of an electron. The emitted positrons react with the electrons of the surrounding matter and lead to characteristic annihilation radiation at 511 keV.

When ^{22}Na decay to excited ^{22}Ne state, energy is being released for ^{22}Ne to go to its ground state. The third peak result from the energy released when the excited neon decay to its ground state. A very small part (0.06 %) of the decays leads directly to the ground state of neon. The rest leads to an excited state of neon, partly via electron capture (9.5 %) from the inner atomic shell, but mainly via positron emission. The excited neon state passes into the ground state whereby a 1275 keV γ quantum is emitted. The lifetime of this excited neon is only 3.7 ps.

^{65}Zn was also positioned 40 cm away from the detector using the same geometry and the detector recorded the spectrum of the unattenuated beam produced by ^{65}Zn for 10 minutes. Figure 4.3 shows the spectrum recorded by the detector. The first two peaks are due to noise, Compton edge, and X-rays. The third

peak is the annihilation peak due to pair production of the main photopeak ($E\gamma$ > 1.022MeV). The fourth is the main photopeak at 1115.54 keV. Zn-65 is a beta emitter that also emits a gamma photon centered around 1115.5 keV. The peaks matche the standard and agreed with the spectrum for ^{65}Zn.

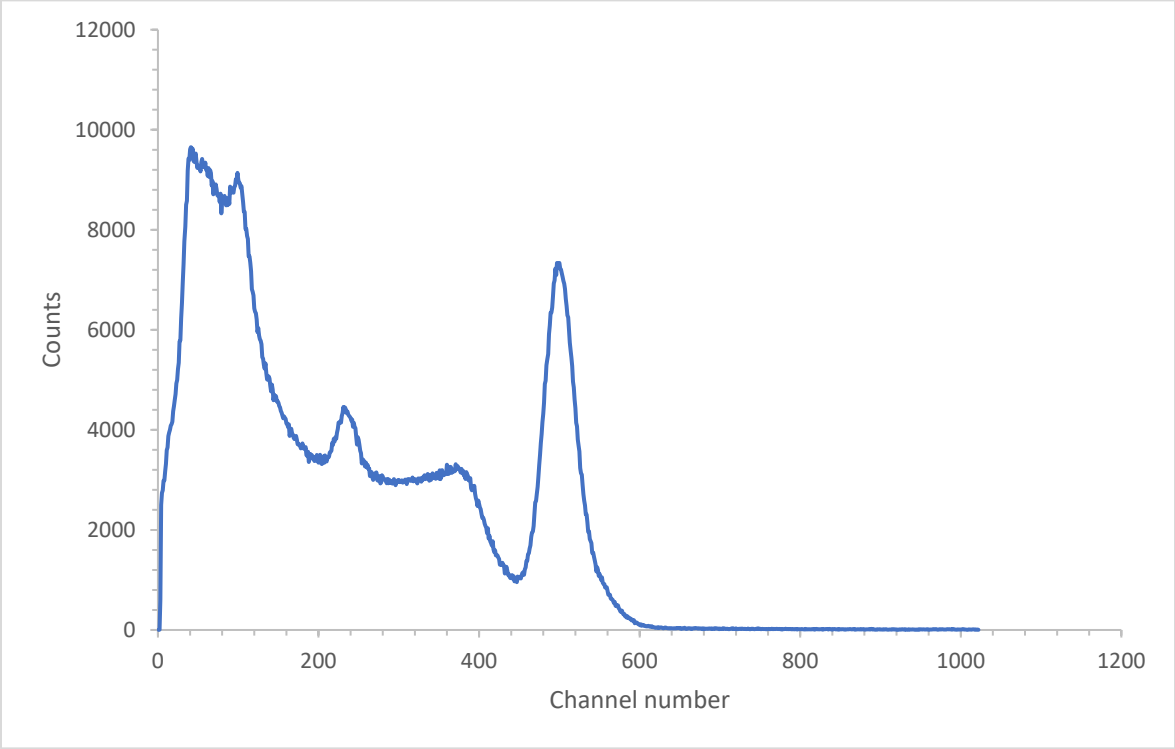

Figure 4.3: Spectrum of ^{65}Zn

4.1.1 NaI detector energy calibration

Equation 3.3 was used to find the scaling factor α for the energy channels, the scaling factor was found to be α = 2.265 from the fit parameter for ^{22}Na peaks. This was used for the corrected spectrum of ^{22}Na in figure 4.4. The photo peaks match the expected energy peaks from ^{22}Na with the corrected energy channel. The

first peak was centered on 511 keV, and the second peak was centered on 1270.71 keV.

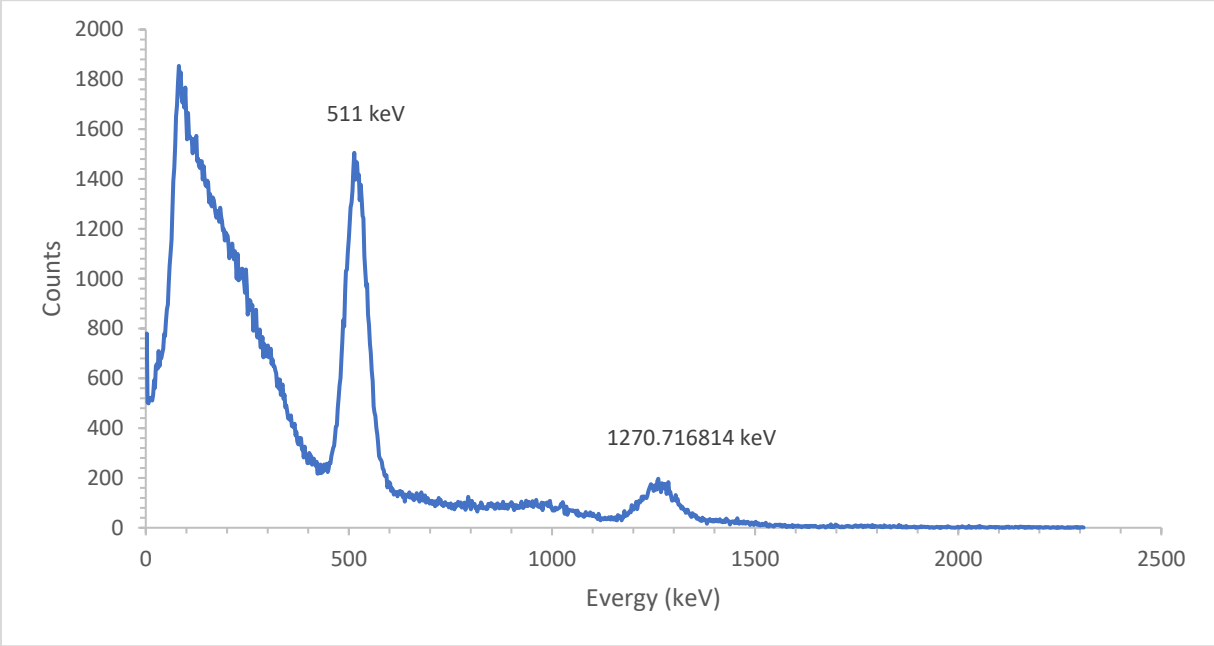

Figure 4.4: Corrected spectrum of ^{22}Na

The corrected spectrum of ^{65}Zn is presented in figure 4.5. The scaling factor above was used to determine the energy channel using equation 3.3. The peaks due to gamma rays from ^{65}Zn were centered of 512.9 keV and 1115 keV, respectively.

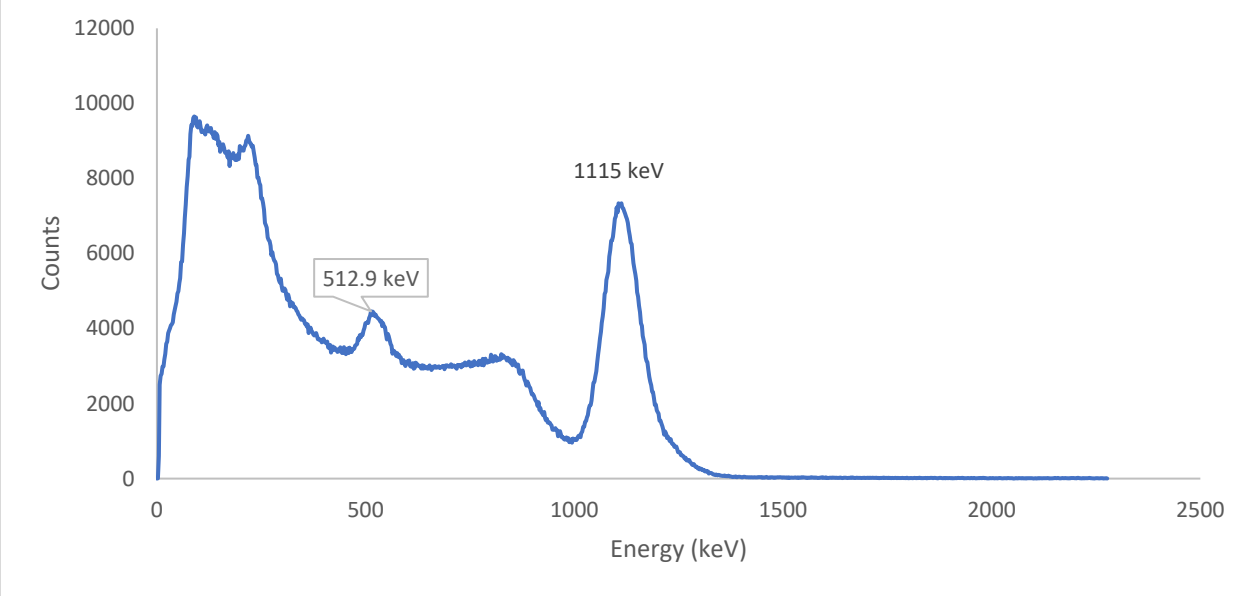

Figure 4.5: Corrected ^{65}Zn spectrum

Figure 4.6 shows the correlation between the channel number and energy. There were only two energy peaks from the ^{22}Na spectrum, and a peak was used from the ^{65}Zn sample source. Hence, three plotted points on the graph. It was observed that the trend line passes close to the origin of the graph and shows a good correlation between the channel number and energy calibration.

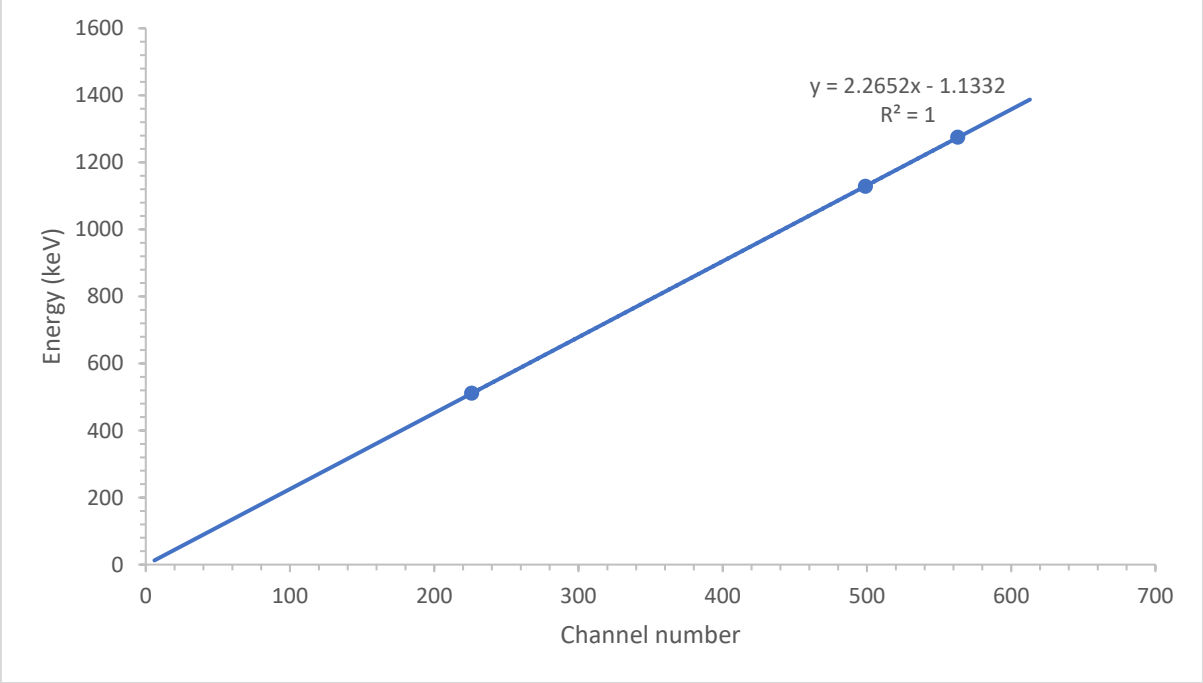

Figure 4.6: Correlation between energy (keV) and channel number

4.1.2 Detector resolution

The detector resolution was calculated using equation 3.1 and its uncertainty was calculated using equation 3.2. For the ^{22}Na source sample, the detector resolution was found to be 13 ±1 % at 511 keV, and the resolution at 1275 keV was found to be 6.92 ± 0.04 %. For the ^{65}Zn source sample, the resolution at 1115 keV was 9.8 ±0.6 %. The resolution of the detector decreases with an increase in photon energy.

4.1.3 Efficiency calibration

The efficiency of the detector was calculated using equation 3.4. Using the energy level of ^{22}Na at 511 keV the efficiency was 0.02 for the source-detector

geometry that was used for this experiment. At 1275 keV, the efficiency was 0.00712 and the geometry was kept the same throughout the experiment. It was noticed that the efficiency decreases with an increase in photon energy. The small efficiency number at 1275 keV is due to the source-detector geometry. The distance between the sample source and the detector was 40 cm, and the detector was also collimated to 4 cm x 4 cm (1.8 in x 1.8 in).

The efficiency of the NaI detector from this experiment was also compared with values from other experiments (Yalcin, et al. 2007) with different geometry but close energy levels. This is presented in table 4.1. The efficiency result from the work of Yalcin *et al* 2007 was interpolated between 320 keV and 662 keV to find the expected value of efficiency at 511 keV. The interpolated value was 0.022 compared to 0.02 calculated using data from this work. The percentage difference between them is 9.1% which is a small number, even though, the geometry was different, considering the distance between the sample source and detector, and collimation of the detector. However, at 1275 keV energy level, the efficiency was much lower than the neighboring energy level. From the work of Yalcin et al 2007, interpolating between 662 keV and 1330 keV to get the expected value for 1275 keV, the expected efficiency was 0.0167 compared to 0.00712 calculated using data from this work. The effects of the geometry were noticed more at 1275 keV energy level having a percentage difference of 57.3% which is a large number compared to the energy level at 511 keV.

Table 4.1: Comparison between total efficiency values for a 7.62 cm x 7.62 cm NaI detector with a point source located *d* = 10.0 cm away from the front face of the detector with this present work

Energy (keV)	Total Efficiency					
	Present work	(Yalcin, et al. 2007)	(Cesana and Terrani 1977)	(Heath 1964)	(Bellusconi, et al. 1974)	(T. Nakamura 1972)
320		0.0249	0.0251	0.0247	0.0250	
511	0.02					
662		0.0202	0.0201	0.0198	0.0190	0.0183
1275	0.00712					
1330		0.0164	0.0165	0.0162	0.0164	0.0168
2620		0.0140				0.0132
2750		0.0139			0.0141	

4.2 Activity of ^{65}Zn

The activity of ^{65}Zn was calculated using equation 3.6 and the manufacturer's value at the time it was used in our department. The activity was verified using the efficiency value of our system at the 1275 keV peak of ^{22}Na with the 1115 keV energy level of ^{65}Zn and the percentage yield of the 1115 keV photon. Since the efficiency of the detector reduces with an increase in photon energy, the efficiency at 1275 keV of the ^{22}Na sample source is the closest we could use to determine the activity of ^{65}Zn at 1115 keV energy level. Table 4.2 shows the results of both the calculated activity and the experimentally evaluated activity with their

percentage difference. The dead time correction was also done using equation [4.1] for the count at 1115 keV of ^{65}Zn, because the dead time was 29.9%, which is a large number and it was due to the activity level of ^{65}Zn compared to ^{22}Na activity level.

$$R_o = R_t(\frac{\%\ dead\ time}{100} + 1) \qquad [4.1]$$

where R_o is the expected count rate without dead time, and R_t is the recorded count rate with the dead time.

Table 4.2: Calculated and experimental activities of ^{65}Zn with the percentage difference

Element	Calculated Activity (MBq)	Experimental Activity (MBq)	Percentage difference (%)
^{65}Zn	38.33	37.36	2.5

4.3 Radiation doses rate

The measured radiation dose rates and the calculated radiation dose rates using equation 3.9 are presented in Table 4.3. These values are compared with the values of the online radprocalculator.

Table 4.3: Radiation dose rate at 2 cm and 10 cm from the sample source

	The dose rate at 2 cm from the sample source (mrad/hr)	The dose rate at 10 cm from the sample source (mrad/hr)
Measured dose with the dosimeter	1789.17	63.30
Calculated dose	1721.51	62.16
Radprocalculator	1161.86	46.46

At 2 cm away from the radioactive source, the percentage difference between the experimental value and the calculated value is 3.7%. This is a very small number. However, doses from high energy beta particles coming from the source sample might have made the difference. At 10 cm the percentage difference is 1.8%. The difference is lesser compare to when the sample source was at 2 cm. This may be due to the attenuation of most of the low energy X-rays and high energy beta particles in the air before getting to the dosimeter. Theoretically, we expect the dose to fall off with the square of the separation between the sample source and the dosimeter, this was observed in the values obtained for both experimental and calculated values.

For the online radprocalculator, the percentage difference between the experimental value and the value from the online radprocalculator at 2 cm separation is 35% this difference is very significant. It was discovered that the online radprocalculator does not consider doses from X-rays from the sample

source, rather it only accounted for radiation doses due to the gamma radiation. Relying solely on the online calculator will not give the exact radiation dose rate at a specific point close to the source because of the doses from the X-rays. At 10 cm away from the sample source, the percentage difference between the experimental and the online radprocalculator is 26.6%. The percentage difference keeps reducing with distance and it may be due to the attenuation of some of the low energy X-rays and beta particles from the sample source with an increase in distance from the source.

4.4 Cumulative dose to fruit flies

The doses to each generation of the fruit flies were calculated using equation 3.10. The fruit flies were irradiated from the egg stage through larvae till the imago stage. The doses were delivered throughout the reproductive cycle of each generation of the fruit flies. This was done continuously for different generations of the flies and the temperature was kept at 25^{o}C. The generations, number of days of irradiation, and doses delivered are presented in table 4.4.

From table 4.4, The doses delivered to the fruit flies keep reducing with each generation except for the 2nd generation that was fairly more than the dose during the 1st generation, the 6th generation which was also fairly more than the 5th generation, and the 8th generation was irradiated for six day. The average reproductive cycle of fruit flies is about 10 days when the temperature is about 25^{o}C and about 14 to 15 days when the temperature is about 20^{o}C. This clearly

shows that temperature is a huge factor during the reproductive life cycle of the fly. The control flies for each generation were kept under identical condition in the same room and shielded from radiation.

Table 4.4. The average dose to each generation of the fruit flies

Generations	Number of days	Hours of irradiation	Range of dose rate in the tube (rad/hr)	Average Volume dose rate (rad/hr)	Total Average volume dose (rad)
1st	9	216	2.344664 - 0.133712	0.887917365	191.7902
2nd	10	238.73	2.227817 - 0.127049	0.843667687	201.4088
3rd	10	238	2.116793 - 0.120717	0.801623208	190.7863
4th	9	216.41	2.00559 - 0.114376	0.759513944	164.3664
5th	9	216	1.889481 - 0.107754	0.715540844	154.5568
6th	10	238	1.800424 - 0.102675	0.681815219	162.272
7th	10	233.58	1.715565 - 0.097836	0.649679186	151.7521
8th	6	150.5	1.630069 - 0.09296	0.617302193	92.90398
9th	10	237	1.566529 - 0.089336	0.593239788	140.5978
10th	9	215	1.484239 - 0.084644	0.562076905	120.8465

Throughout the experiment, the temperature was kept fairly the same at 25^{o}C for consistency. The average volume dose rate for the whole generations was 0.71 ±0.03 rad/hr. The total average dose delivered to the whole generations was 160 ±10 rad. The ranges of dose rate within the test tube falls sharply with increase in distance. This shows how distance can greatly affect radiation dose rate at a

specific point. The range distance was between 0.3 cm and 6.7 cm for all the generations of flies considering the dimension of the test tubes.

In other experiments carried out in the same laboratory with just three generations, the first generation of fruit flies was irradiated for 7 days. The other two generations of this experiment have life cycles of 13 and 10 days, respectively. The average cumulative dose during this period was 270 ±50 rad. In another experiment conducted in the laboratory under the same conditions with just one generation, the reproductive life cycle of the fruit flies was 12 days. The cumulative dose was over the 12 days was 298.10 rad.

CHAPTER FIVE

SUMMARY AND CONCLUSIONS

5.1 Summary and conclusions

The experiment showed that the resolution of the NaI detector decreases with an increase in photon energy and there is a linear dependence between the resolution and the photon energy. This also agreed with some published work by Yalcin, *et al*., 2007. It was also discovered that the efficiency of the detector reduces with an increase in photon energy. The percentage difference of the efficiency of the detector at a higher energy level was off by a large number compared to the percentage difference of the efficiency at a lower energy level. The efficiency value at 1275 keV of ^{22}Na was used to predict the activity of ^{65}Zn using the photon energy at 1115 keV of ^{65}Zn. The predicted activity has a percentage difference of 2.5 % from the calculated value using the manufacturer's value.

The doses rate from ^{65}Zn was measured using thermoluminescent dosimeters at 2 cm and 10 cm from the source. The calculated dose rate at 2 cm has 3.7 % difference from the experimental value while the dose rate at 10 cm has 1.8 % difference from the experimental value. The online radprocalculator dose rate values have larger percentage differences from the experimental values both at 2 cm and 10 cm away from the source. The average time of irradiation was 9 days with an average cumulative dose of 160 ±10 rad.

The data obtained showed that there is a linear relationship between the channel number and energy level. The resolution of the detector reduces with an

increase in photon energy and has a linear correlation. The activity of ^{65}Zn calculated using the detector's efficiency value was very close to the value evaluated using the manufacturer's value. The experimental dose rate and the calculated dose rate showed a good correlation with both obeying the inverse square law.

From the results of this experiment, I will recommend that the online radprocalculator should be reviewed to accommodate for X-rays from the radioactive samples since X-rays also contribute to the dose rates a specific point close to the source. Investigation into the gene expression of the fruit flies should be done and future studies should include inquiries into physical and behavioral changes, life span, and resistance to stress of the offspring of the irradiated flies.

References

Ainsbury, EA, SD Bouffler, and W Dorr. 2009. "Radaition cataractogenesis: A review of recent studies." *Radiat Res* 172: 1-9.

Alession, N, S Gaudio, and S Capasso. 2015. "Low dose radation induced senescence of human mesenchymal stromal cells and impaired the autography process." *Omcotarget* 6: 8122 - 8166.

Anne, PR. 2002. "Phase II trial of subcutaneous amisfostine in patients undergoing radiation therapy for head and neck cancer." *Semin Oncol* 29: 80-83.

Anonymous. 1991. "Recommendations of the International Commission of Radiological Protection." *ICRP Publications.* Annuals of ICRP. 1-3.

Antosh, M, D Fox, T Hasselbacher, R Lanou, N Neretti, and LN Cooper. 2014. "Drosophila Melanogaster show a threshold effect in response to radiation." *dose response* 551-581. doi:10.2203/dose-response.13-047.Antosh.

Bellusconi, M, R Deleo, A Pantaleo, and A Vox. 1974. "Efficiencies and response functions of NaI(T1) Crystals for gamma rays from thick disk sources." *Nud Instrum Methods* 553-563.

Bier, E. 2005. "Drosophila, the golden bug, emerges as a tool for human genetics." *Nature Reviews Genetics* 6: 9-23.

Bonner, WM. 2003. "Low-dose radiation: Thresholds, bystander effects, and adaptive responses." *proc Natl Acad Sci USA* 100: 4973-4975.

Cesana, A, and M Terrani. 1977. "Gamma-ray activity determination in large volume samples with Ge-Li detector." *Anal. Chem* 1156-1159.

Coleman, MA, E Yin, and LE Peterson. 2005. "Low-dose irradiation alters the transcript profiles of human lymphoblastoid cells including genes associated with cytogenetic radioadaptive response." *radiat Res* 164: 369-382.

FDA. 2015. "U.S. Food and Drug Administration. Radiation Quantities and units." http://www.fda.gov/Radiation-EmittingproductsandProcedures/MedicalImaging/MedicalX-rays/ucm115335htm.

FDA. 2015. *US Food and Drug Administration: Radiation quantities and units.* www.fda.gov.

Hall, EJ, and AJ Giaccia. 2011. "Radiobiology for the radiologist." *Lippincott Williams & Wilkins, Philadelphia* 7th Edition.

Heath, RL. 1964. "Scintillat ." *Spectrom.*

Hou, SX, and SR Singh. 2017. "Stem-cell based tumorigenesis in adult Drosophila." *Curr Top Dev Biol* 121: 311-337. doi:10.1016/bs.ctdb.2016.07.013.

ICRP. 1991. "1990 Recommendations of International Commission on Radiological Protection." *Ann ICRP* 21: 1-201.

—. 2000. "International Commission on Radiological Protection. Pregnancy and medical radiation." *ICRP.* Ann ICRP. 1-43.

ICRP. 2007. *The 2007 recommendations of the International Commission on Radiological Protection.* ICRP.

—. 2007. "The recommendations of the international commission on radiological protection." *ICRP publication.* Ann ICRP. 1-332.

Ikushima, T, H Aritomi, and J Morisita. 1996. "radioadaptive response: efficient repair of radiation-induced DNA damage in adapted cells." *Mutat Res* 193-198.

Ina, Y, H Tanooka, and T Yamada. 2005. "Suppression of thymic lymphoma induction by life-long low-dose-rate irradiation accompanied by immune activation in C57BL/6 mice." *Radiat Res* 153-158.

Johnson, WA, and JW Carder. 2012. "Drosophila nociceptors mediate larval aversion to dry surface environments utilizing both painless TRP channel and the DEG/ENaC subunit, PPK1." *PLos One* 7: 328-378.

Keum, DK, I Jun, KM Lim, and YH Choi. 2010. "Absorbed internal dose conversion coefficiets for domestic reference animals and plant." *Nuclear Engineering and Technology* 42: 89-96.

Kohler, RE. 1994. *Lords of the fly: Drosophila genetics and the experimental life.* Chicago: University of chicago press.

Koturbash, I., K. Kutanzi, K. Hendrickson, R. Rodriguez Juarez, D. Kogosov, and O. Kovalchuk. 2008. "Radiation-induced bystander effects in vivo are sex specific." *Mutation Research* 28-36.

Kreso, A, and JE Dick. 2014. "Evolution of the cancer stem cell model." *Cell Stem Cell* 14: 275-291. doi:10.1016/j.stem.2014.02.006.

Little, J.B. 2003. "Genomic instability and bystander effects: a historical perspective." *Oncogene* 22: 6978-6987.

Malanchi, I, A Santamaria-Martinez, E Susanto, H Peng, HA Lehr, and JF Delaloye. 2011. "Interactions between cancer stem cells and their niche govern mestastatic colonization." *Nature* 481: 85-89. doi:10.1038/nature10694.

Marples, B, BG Wouters, and AL Collis SJ et. 2004. "Low dose hyper-radiosensitivity: a consequence of ineffective cell cycle arrest of radiation-damaged G2-phase cells." *Gadiat Res* 161: 247-255.

Mattson, MP. 2008. "Hormesis defied." *Ageing Res Rev* 7: 1-7.

Moller, AP, and TA Mousseau. 2013. "The effects of natural variation in background radioactivity on humans, animals, and other organisms." *Bio Rev Camb Philos Soc.* 226-254.

Morgan, W.F, and W.J Bair. 2013. "Issues in low dose radiation biology: the controversy continues. A perspective." *Radiation Research* 179: 501-510.

Moskalev, A, M Shaposhnikov, A Snezhkina, V Kogan, E Plyusnina, and D Peregudova. 2014. "Minning gene expression data for pollutants (dioxin, toluene, formaldehyde) and low dose of gamma-irradiation." *PLoS One* 9 (1). doi:10.1371/journal.pone.0086051.

Moskalev, A, M Shaposhnikov, and E Turysheva. 2009. "Life span alteration after irradiation in Drosophila Melanogaster strains with mutations of Hsf and Hsps." *Biogerontology* 10: 3-11. doi:10.1007/s10522-008-9147-5.

Moskalev, AA, EN Plyusnina, and MV Shaposhnikov. 2011. "Radiation Hormesis and radioadaptive response in Drosophila Melanogaster flies with different genetic backgrounds: the role of cellular stress-resistance mechanisms." *Biogerontology* 12: 253-63. doi:10.1007/s10522-011-9320-0.

Moskalev, AA, EN Plyusnina, and MV Shaposhnikov. 2011. "Radiation hormesis and rdioadaptive response in Drosophila melanogaster flies with different genetic backgrounds: the role of cellular stress-resistance mechanisms." *Biogerontology* 12: 253-263.

Mueller, MT, PC Hermann, J Witthauer, B Rubio-Viqueira, SF Leicht, and S Huber. 2009. "Combined targeted treatment to eliminate tumorigenic cancer stem cells in human pancreatic cancer." *Gastroenterology* 137: 1102-1113. doi:10.1053/j.gastro.2009.05.053.

Muller, HJ. 1928. "The production of mutations by X-rays." *Natl Acad Sci USA* (Natl Acad Sci USA) 14: 714.

Nakamura, N, A Suyama, A Noda, and Y Kodama. 2013. "Radiation effects on human heredity." *Annu Rev Genet* 47: 33-50. doi:10.1146/annurev-genet-111212-133501.

Nakamura, N, A Suyama, A Noda, and Y Kodama. 2013. "Radiation effects on human heredity." *Annu Rev Genet.* 47: 33-50.

Nakamura, T. 1972. "Monte-Carlo claculation of efficiencies and response functions of NaI(T1) crystals for thick disk gamma-ray sources and its application to Ge(Li) detectors." *Nuclear Instrum Methods* 77.

O'Driscoll, M, and PA Jeggo. 2006. "The role od double-strand break repair - insight from human genetics." *Nat RevGenet* 7: 45-54.

Ogaki, M, and E Nakashima- Tanaka. 1966. "Inheritance of radioresistance in Drosophila." *I. Mutat Res* 3: 438-443.

Ogaki, M, and E Nakashima-Tanaka. 1966. "Inheritance of radioresistance in Drosophila." *I. Mutat Res.* 3: 438-443.

Paaby, AB, and PS Schmidt. 2009. "Dissecting the genetics of longevity in Drosophila melanogaster." *Landes Bioscience* 3: 29-38.

Parashar, V, S Frankel, AG Luriec, and B Rogina. 2008. "The effects of age on radiation resistance and oxidatve stress in adult." *Drosophila melanogaster. Radation Research* 169: 707-711.

Prasad, KN, WC cole, and GM Hasse. 2004. "Radiation Protection in humans: extending the concept of as low as reasonably achievable (ALARA) from dose to biological damage." *The british journal of radiology* 77: 97-99.

Prasad, KN, WC Cole, B Kumur, and K Che Prasad. 2002. "Pros and cons of antioxidant use during radiation therapy." *Cancer Treat Rev* 28: 79-91.

Prise, KM, and A Saran. 2011. "Concise review: Stem cell effects in radiation risk." *Stem Cells* 29: 1315 - 1321.

Rando, TA. 2006. "Stem cells, ageing and the quest for immortality." *Nature 2006* 411: 1080 - 1086.

Roost, E, E Funck, A Spernol, and R Vaninbroukx. 1972. "The decay of 65Zn." *Zeitschrift fur Physik* 5: 395 - 412.

Rothkamm, K, and M Lobrich. 2003. "Evidence for a lack of DNA double-strand break repair in human cells exposed to very low x-ray doses." *Proc Natl Acad Sci USA* 100: 5057-5062.

Saha, GB. 2013. *Radiation biology in physics and radiobiology of nuclear medicine.* New York: Springer Science + Business Media.

Seong, KM, SW Seo, HY Jeon, BS Lee, and SY Nam. 2011. "Genome-wide analysis of low-dose irradiated male Drosophila melanogaster with extended longevity." *Biogerontology* 12 (2): 94-107. doi:10.1007/s10522-010-9295-2.

Shahbazi-Gahrouei, D, M Gholami, and S Setavandeh. 2013. "A review on natural background radiation." *Biomed Res* 65.

shaw, P, P Crouail, and F Drouet. 2010. "Risk-assessment and continuous improvement programmes." *Radioprotection* 25: 401-408.

Sistrom, CL. 2008. "In support of thr ACR appropriateness criteria." *J Am Coll Radiol* 5: 630-635.

Tang, FR, and WK Loke. 2015. "Molecular mechanisms of low dose ionizing radiation-induced hormesis, adaptive responses, radioresistance, bystander effects, and genomic instability." *Int J Radiat Biol* 91: 13-27.

1946. *The nobel prize in Physiology or medicine.* Nobelprize. doi:http://www.nobelprize.org/nobelprizes/medicine/laureates/1946/.

1933. *The Nobel Prize in Physiology or Medicine.* Nobelprice.org. http://www.nobelprize.org/nobelprizes/medicine/laureates/1933/.

Tubianna, M. 2009. "Prevention of cancer and the dose-effect relationship: the carcinogenic effects of ionizing radiations." *Cancer Radiotherapy* 13: 238-258.

Ugur, B, K Chen, and HJ Bellen. 2016. "Drosophilia tools and assays for the study of human diseases." *Dis Model Mech* 9: 235-244. doi:10.1242/dmm.023762.

Vaiserman, AM, NM Koshel, AY Litoshenko, TG Mozzhukhina, and VP Voitenko. 2003. "Effects of X-rays irradiation in early ontogenesis on the longevity and amount of the S1 nuclease-sensitive DNA sites in adult Drosophila Melanogaster." *Biogerontology* 4: 9-14.

Wardman, P. 2009. "The importance of radiation chemistry to radiation and free radical biology." *British Journal of Radiology* 89 - 104.

Weizman, N, Y Shiloh, and A Barzilai. 2003. "Contribution of the Atm protein to maintaining cellular homeostatis evidence by continuous activation of the AP-1 pathway in Atm-deficient brains." *J Biol Chem* 278: 6741-6747.

Win, DT, and M Al Masum. 2003. "Weapons of Mass Destruction." *Assumption University Journal* 6: 199-219.

Wrixon, A.D. 2008. "New ICRP recommendations." *Journal of Radiological Protection.* 28: 161-168.

Y, Ina, and Sakai K. 2004. "Prolongation of life span associated with immunological modification by chronic low-dose-rate irradiation in MRL-lpr/lpr mice." *Radiat Res* 161: 168-173.

Y, Ina, Tanooka H, and Yamada T. 2005. "Suppression of thymic lymphoma induction by life-long low-dose-rate irradiation accompanied by immune activation in C57BL/6 mice." *Radiat Res* 163: 153-158.

Yalcin, S, O Gurler, G Kaynak, and O Gundogdu. 2007. "Calculation of total counting efficiency of a NaI(T1) detector by hybrid Monte-Carlo method for point and disk sources." *Elservier* 1179-1186.